

# We are IntechOpen, the world's leading publisher of Open Access books Built by scientists, for scientists

**4,800**

Open access books available

**122,000**

International authors and editors

**135M**

Downloads

Our authors are among the

**154**

Countries delivered to

**TOP 1%**

most cited scientists

**12.2%**

Contributors from top 500 universities



**WEB OF SCIENCE™**

Selection of our books indexed in the Book Citation Index  
in Web of Science™ Core Collection (BKCI)

Interested in publishing with us?  
Contact [book.department@intechopen.com](mailto:book.department@intechopen.com)

Numbers displayed above are based on latest data collected.

For more information visit [www.intechopen.com](http://www.intechopen.com)



# Modeling and Simulation of Water Gas Shift Reactor: An Industrial Case

Douglas Falleiros Barbosa Lima<sup>1</sup>, Fernando Ademar Zanella<sup>1</sup>,  
Marcelo Kaminski Lenzi<sup>2</sup> and Papa Matar Ndiaye<sup>2</sup>

<sup>1</sup>Refinaria Presidente Getúlio Vargas – REPAR / PETROBRAS

<sup>2</sup>Universidade Federal do Paraná – UFPR  
Brazil

## 1. Introduction

Recently, refineries finished products hydro treatment became critical due to changes in fuel regulations. These changes are related to the specification of more clean fuels with special focus in sulfur content reduction. In order to achieve these goals more hydro treatment is needed. Hydrogen is the main raw material to hydro treatment units.

In refining plants, a hydrogen generation unit usually is necessary to supply the hydrogen demand to all demanding processes.

The process known as steam reform unit is the most widely adopted technology. In large scale, it has the highest energetic efficiency and the best cost-benefit ratio (Borges, 2009).

In this process the hydrogen conversion is carried out in two reactors in series. The first one, the steam reform reactor converts steam and a hydrocarbon (naphtha or natural gas) into *syngas*. In the sequence, a reactor known as water gas shift reactor (WGSR) converts the carbon monoxide present in *syngas* into carbon dioxide and more hydrogen is generated.

Consequently, the WGSR, an intermediate step of hydrogen generation process, plays a key role in a petrochemical plant due to hydrogen increasing demand.

### 1.1 Hydrogen generation unit

The hydrogen generation unit, based on the steam reform technology, is responsible for approximately 95% of generated hydrogen (Borges, 2009).

A simplified unit block diagram is showed in figure 1.1.1.

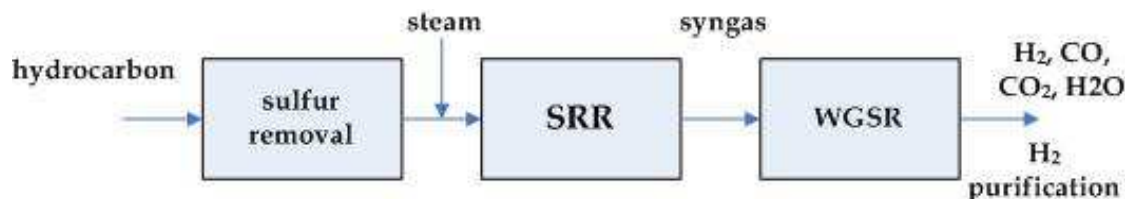
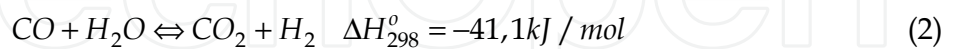
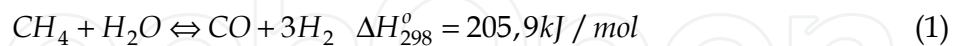


Fig. 1.1.1. Hydrogen generation unit – process block diagram.

First, sulfur is removed from the hydrocarbon stream (usually natural gas), in order to prevent catalyst poisoning and deactivation with the use of a guard bed. Steam is mixed in the main stream in a fixed steam to carbon molar basis. The steam reform reactor (SRR) is a multitubular catalyst filled furnace reactor where the hydrocarbon plus steam are converted into syngas at high temperatures (700°C - 850°C) according to the following reaction:



The reaction (1) is endothermic and reaction (2) is moderately exothermic. Both are reversible reactions. In the SRR, (1) is the main reaction and generates most of the hydrogen. The reaction (2) due to its endothermic nature occurs in a lower extension in the SRR. The syngas stream composition is CO and H<sub>2</sub>, in this process CO<sub>2</sub> and H<sub>2</sub>O are also present in gas state. The main purpose of the water gas shift reactor (WGSR) is to carry out the reaction (2) reducing the CO fraction and increasing the hydrogen yield. Finally, the WGSR stream is conducted to a purification section, where hydrogen purity is increased according to the process needs.

## 2. The water gas shift reaction

### 2.1 kinetic rate expression

The water gas shift reaction (reaction 2) is a heterogeneous reaction (gas/solid).

According to (Smith et al., 2010) in this kind of application, there are two options in the WGSR step. Using a high temperature shift (HTS) catalyst based reactor or a series of HTS followed by a low temperature shift catalyst based reactor (LTS) with intercooling stage to increase the overall conversion and high purity hydrogen is needed (Newsome, 1980).

The chapter focuses on a HTS ferrochrome catalyst industrial reactor modeling.

The HTS usually is an iron oxide - chromium oxide based catalyst. Also reaction promoters such as Cu may be present in catalyst composition. Operational temperatures vary from 310°C to 450°C. Inlet temperatures are usually kept at 350°C to prevent the catalyst bed temperature from damage. Exit CO concentrations are in the order of 2% to 4%. Industrial reactors can operate from atmospheric pressure to 8375 kPa. Sulfur is a poison for Fe-Cr catalysts.

LTS reactors are copper based catalyst. Typical compositions include Cu, Zn, Cr and Al oxides.

Recent catalysts can be operated at medium temperatures around 300°C. Copper is more sensitive to catalyst thermal sintering and should not be operated at higher temperatures. Sulfur is also a poison to LTS reactors. Typical exit concentration is of 0,1% of CO.

The reaction is operated adiabatically in industrial scale, where the temperature increases along the length of the reactor.

According to Arrhenius law of kinetics, increasing temperature increases the reaction rate. By the other side, the thermodynamic of equilibrium or Le Châtelier principle states that increasing the temperature of an exothermic reaction shifts the reaction to reactants side decreasing its equilibrium conversion. Therefore the water gas shift reaction is a balance between these effects and the reactor optimal operational point takes into account the tradeoff between kinetics and equilibrium driving forces.

In (Chen et al., 2008) experimental data indicates that increasing temperature in HTS will promote the performance of WGSR. For the LTS, the reaction is not excited if the reaction is bellow 200°C. Once the temperature reaches 200 °C the reaction occurs, but the CO conversion decreases with increasing temperature. This fact reveals that that the water gas shift reactions with the HTS and the LTS are governed by chemical kinetics and thermodynamic equilibrium, respectively in industrial conditions.

(Smith et al., 2010) classifies the reaction kinetic models in microkinetic approach and the empirical method.

Basically, the micro kinetic approach explores the detailed chemistry of the reaction. On the other hand, the empirical models are based on the experimental results and are typically expressed in the Arrhenius model and provide an easy and computationally lighter way to predict the rate of reaction. The main disadvantage is the fact that the adjusted model cannot be extrapolated to different composition and types of catalysts.

Many empirical expressions have been reported in literature for HTS. (Newsome, 1980) and (Smith et al., 2010).

An empirical rate expression succesfully used to describe the WGSR in ferrochrome catalysts is a power law type: (Newsome, 1980)

$$r = k_0 \cdot e^{\frac{-E_a}{RT}} \cdot P_{CO}^l \cdot P_{H_2O}^m \cdot P_{CO_2}^n \cdot P_{H_2}^q \cdot \left( 1 - \frac{1}{K_{eq}} \cdot \frac{P_{CO_2} \cdot P_{H_2}}{P_{CO} \cdot P_{H_2O}} \right) \quad (3)$$

Where:

r - reaction rate.

E<sub>a</sub> - activation energy.

K<sub>o</sub> - pre exponential factor.

K<sub>eq</sub> - reaction equilibrium constant.

l, m, n, q - estimated parameters by experimental data.

P<sub>y</sub> - partial pressure of component y.

R - universal gases constant.

T - absolute temperature.

The reaction equilibrium constant derived from thermodynamics as function of temperature is given by (Smith et al., 2010):

$$\ln(K_{eq}) = \frac{5693,5}{T} + 1,077 \cdot \ln(T) + 5,44 \cdot 10^{-4} \cdot T - 1,125 \cdot 10^{-7} \cdot T^2 - \frac{49170}{T^2} - 13,148 \quad (4)$$

T - temperature in Kelvin.

Several authors have published estimated parameters for specific catalysts types or catalysts classes. (Newsome, 1980) and (Smith et al., 2010)

Table 2.1.1 summarizes some previous published values and authors for HTS catalysts:

Author	Catalyst information	$K_0$	$E_a$ (kJ/mol)	$l$	$m$	$n$	$q$
Bohlbro et al. (Newsome, 1980)	Fe <sub>2</sub> O <sub>3</sub> / Cr <sub>2</sub> O <sub>3</sub> Commercial reduced particle size	-	105,9	0,93	0,24	-0,31	0,00
Bohlbro et al. (Newsome, 1980)	Fe <sub>2</sub> O <sub>3</sub> / Cr <sub>2</sub> O <sub>3</sub> Commercial Large particle size	-	59,8	0,87	0,26	-0,18	0,00
S.S. Hla et al. (Hla et al., 2009)	Fe <sub>2</sub> O <sub>3</sub> / Cr <sub>2</sub> O <sub>3</sub> /CuO type 1	10 <sup>2,845</sup>	111	1	0	-0,36	-0,09
S.S. Hla et al. (Hla et al., 2009)	Fe <sub>2</sub> O <sub>3</sub> / Cr <sub>2</sub> O <sub>3</sub> /CuO type 2	10 <sup>0,659</sup>	88	0,9	0,31	-0,156	-0,05
Adams and Barton. (Adams & Barton, 2009)	Fe <sub>2</sub> O <sub>3</sub> / Cr <sub>2</sub> O <sub>3</sub> /CuO Commercial type 1 Same as Hla et al.	725	110	1	0	-0,32	-0,083

Table 2.1.1. Estimated parameters for power law HTS catalysts.

In industrial reactors, catalysts are loaded in pellets. Therefore, intrinsic rate expressions cannot be used in pseudo-homogeneous models without some type of compensation to account for diffusion effects.

According to (Newsome, 1980) two different methods can be applied to model industrial reactors as pseudo-homogeneous reactions. The first was proposed by Bohlbro and Jorgensen consists of estimating the empirical rate expression in laboratory using commercial size catalysts. The diffusion effects remain implicit in the rate expression. First and second rows of Table 2.1.1 illustrate this method. The catalyst in the first row was grounded to avoid diffusion effects. In the second row the same catalyst was used in commercial pellet size. It can be noted slight differences between  $l$ ,  $m$ ,  $n$  e  $q$  parameters. The disadvantage of this method is that the rate expression can model successfully only a reactor with this specific type and size of catalyst.

(Hla et al., 2009) estimates the intrinsic rate parameters for two commercial catalysts as can be seen in rows three and four.

(Adams & Barton, 2009) also model a WGS reactor using a heterogeneous modeling approach. The intrinsic rate expression is from Hla et al. previous article. The parameters are result for the best fit estimation.

The second approach of pseudo-homogeneous rate modeling consists of using correction factors to compensate for the pore diffusion phenomena in the catalyst, catalyst age,

operating pressure and hydrogen sulfide concentration with intrinsic rate expressions. (Singh and Saraf, 1977) is a good example of this method.

## 2.2 Mathematical modeling

In this section, mathematical expressions for the fixed bed adiabatic catalytic WGSR fundamental principles (conservation equations) are developed.

A basic ideal flow steady state one-dimensional model is presented.

The differential molar balance simplified to a fixed bed reactor can be expressed as equation 5: (Froment and Bischoff, 1990)

$$\frac{dX_a}{dW} = \frac{r_a}{F_{a0}} \quad (5)$$

$X_a$  - component "a" conversion.

$W$  - catalyst weight.

$r_a$  - rate of reaction of component "a".

$F_{a0}$  - molar feed rate of reactant "a".

$F_a$  - molar flow of component "a" leaving the reactor.

The ideal model assumes that concentration and temperature gradients only occur in the axial direction. The only transport mechanism operating in this direction is the overall flow itself, and is considered to be of the plug flow type.

In case of a reactor bed with a fixed cross sectional area ( $S$ ), the differential molar balance can be rewritten as a function of the reactor differential length as can be seen in equation 6:

$$\frac{dX_a}{dz} = \frac{r_a \cdot \rho_B \cdot S}{F_{a0}} \quad (6)$$

$\rho_B$  - catalyst bulk density.

$S$  - reactor bed constant section area.

$z$  - length of reactor ( $z$  axis - axial direction).

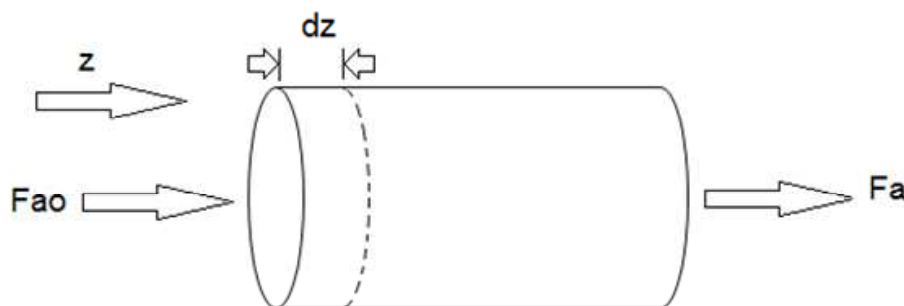


Fig. 2.2.1. Reactor differential volume representation.

The differential equation of energy conservation may be written as equation 7:

$$\sum F_i \cdot C_{pi} \cdot \frac{dT}{dz} = (-\Delta H_R) \cdot r_a \cdot \rho_B \cdot S - 4 \frac{U}{d_t} \cdot (T - T_R) \quad (7)$$

$\Delta H_R$  - enthalpy of reaction.

$C_{pi}$  - specific heat of component "i".

$F_i$  - component "i" molar flow.

$T, T_R$  - reactor temperature and temperature at radius R of internal tube.

$d_t$  - internal tube diameter.

$U$  - overall heat transfer coefficient.

For an adiabatic reactor  $U$  equals zero and equation 3 can be simplified to:

$$\sum F_i \cdot C_{pi} \cdot \frac{dT}{dz} = (-\Delta H_R) \cdot r_a \cdot \rho_B \cdot S \quad (8)$$

The momentum differential equation can be defined as in equation 9:

$$-\frac{dP}{dz} = -f \cdot \frac{\rho_g \cdot u_s^2}{d_p} \quad (9)$$

$P$  - reactor pressure in position  $z$ .

$f$  - friction factor.

$\rho_g$  - gas density.

$u_s$  - superficial velocity.

$d_p$  - particle diameter.

The aim of the next topics is to develop this set of equations to model an industrial high temperature WGSR.

## 2.3 Some design aspects

When designing WGSR (Chen et al, 2008), it is known that a proper selection on certain parameters is of the most importance because the reaction result depends strongly on the combination of these parameters. Typically, the important parameters include the catalyst type, residence time of reactants in a catalyst bed, reaction temperature and feeding reactants ratio or CO/steam ratio.

### 2.3.1 Types of catalysts

According to the reaction temperature (Chen et al, 2008), the WGSR falls into two categories: high-temperature shift catalyst (HTC) and low-temperature shift catalyst (LTC). The catalyst commonly used in the former is an iron-chromium-based catalyst, whereas a copper-zinc-based catalyst is frequently adopted in the latter.

### 2.3.2 Residence time

It is known that the catalyst amount in a reactor is highly related to the overall project cost. In other words, if a reaction can be developed with least catalyst, both the operation (or



catalyst) cost and the facility (or space) cost can be reduced effectively. The least catalyst amount can be evaluated by determining the residence time of reactants in a catalyst bed.

For both categories of reaction, a residence time of 0.09 s is long enough to establish an appropriate WGSR (Chen et al, 2008), a design factor can be used to compensate deactivation during the catalyst life.

### 2.3.3 Reaction temperature

The reaction temperature on the design of the WGSR, varies according with the type of catalyst used (Chen et al, 2008), For HTC, increasing reaction temperature, the concentration of CO declines with respect to the temperature, thus the conversion of WGSR increases, but between 400°C and 500 °C the change in this propriety is small, so temperatures between 350°C and 400°C the major reaction occur.

In the case of LTC reaction, for temperatures below 150°C, no reaction take place, increasing to 200°C the conversion rise to above 90%. If temperature is increased further the conversion begins to fall. So, an optimal reaction, for the WGSR with the LTC is obtained in temperatures around 200°C.

The WGSR is an exothermic reaction in nature, from thermodynamics it is known that an increase in reaction temperature will impede the forward reaction for H<sub>2</sub> production in the WGSR. Because the behavior, it is realized that the WGSR with the LTC catalyst is governed by chemical equilibrium.

In contrast, for the HTC catalyst, the CO conversion is highly sensitive to the reaction temperature and an increase in temperature is conducive to the hydrogen generation. It follows that the reactions with the HTC are controlled by chemical kinetics (i.e. Arrhenius law).

### 2.3.4 CO/steam ratio

For both kind of catalysts when the CO/steam ratio is large than 1/4, the performance of the WGSR is sensitive the variation of the ratio. Alternatively, if the ratio is smaller than 1/4, varying the ratio merely has a slight influence on the performance(Chen et al, 2008).

## 3. Experimental data

Experimental data of an industrial shift reactor of REPAR/PETROBRAS were used for the modeling studies. The reactor performs CO oxidation to CO<sub>2</sub> using industrial steam. The reaction occurs in a fixed bed filled with a Fe-Cr-based catalyst, which is shown in Figure 3.1.

The historical data set comprises 4 years of operation. More specifically, samples withdrawn from feed and exist streams were analyzed by chromatography, following the technical standard norm (NBR-14903, 2002). Temperature measurements are performed using K type thermocouples connected to Honeywell STT3000 transmitters positioned according to Figure 3.2. Finally, it is important to mention that feed flow rate measurements were performed using orifice plates connected to a Honeywell STD900 differential pressure



transmitter and the reactor pressure drop was measured using manometric pressure coupled to Honeywell STD900 transmitters.



Fig. 3.1. Catalyst.

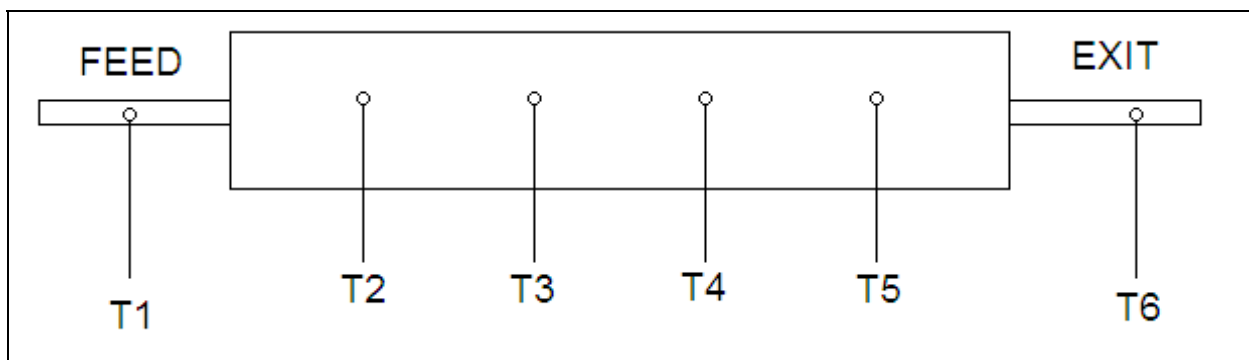


Fig. 3.2. Temperature measurement positioning.

Experimental data of CO conversion are presented in Figure 3.3. These data were normalized by dividing the experimental value by the reactor design conversion value. It is important to state that all experimental data were normalized to the design values in order to avoid numerical convergence issues along the modeling and parameter estimation tasks.

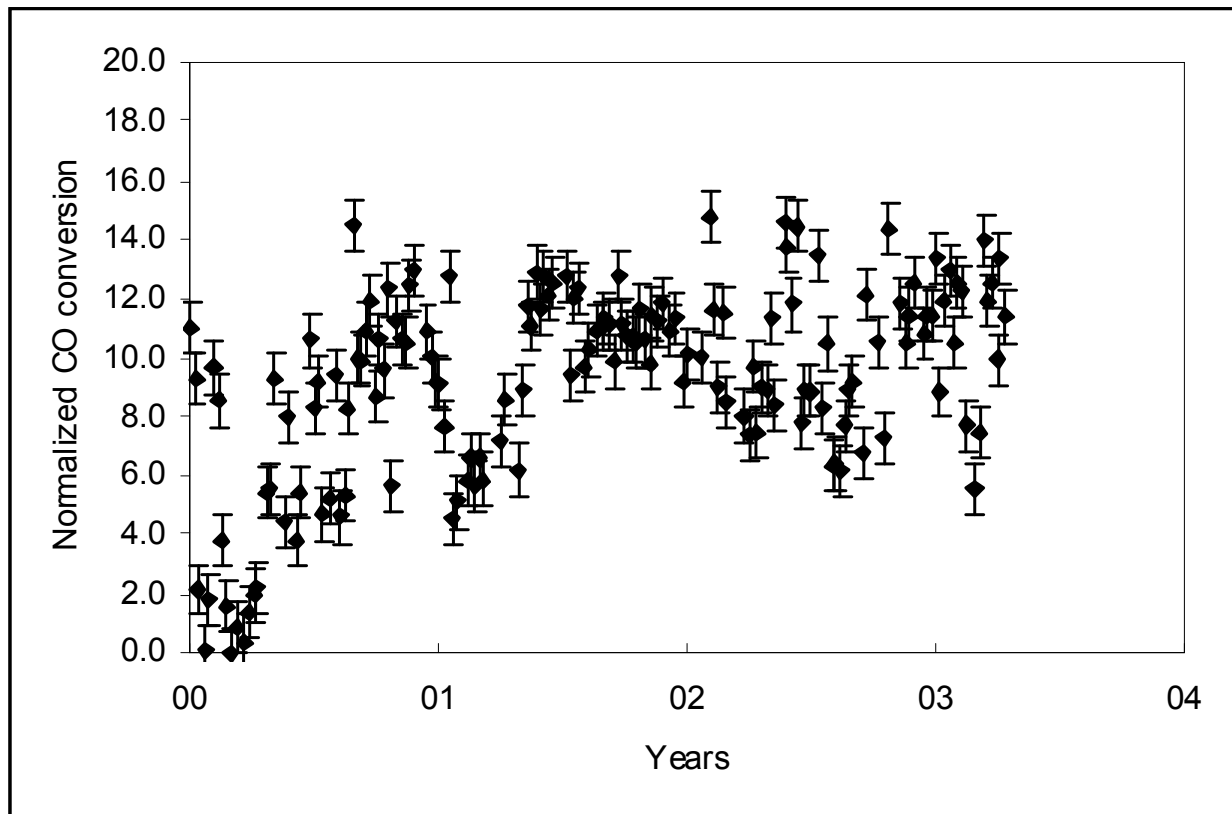


Fig. 3.3. Normalized experimental CO conversion.

The modeling work will focus on CO conversion, however this variable is not directly measured, but actually obtained from chromatographic analysis using Eq. (10), which considers the measurement of CO, CO<sub>2</sub> and CH<sub>4</sub> in the feed and exit streams.

$$X_{\text{CO}} = 100 - 100 * \frac{\text{CO}_s * (\text{CH}_{4e} + \text{CO}_e + \text{CO}_{2e})}{\text{CO}_e * (\text{CH}_{4s} + \text{CO}_s + \text{CO}_{2s})} \quad (10)$$

However, it is important to estimate the experimental uncertainty (*i*) of CO conversion the measurement, i.e., an estimate of the CO conversion variance. This calculation can be done by applying an error propagation approach to Eq. (10), more specifically, an estimate can be obtained by Eq. (11), which considers the variance of CO, CO<sub>2</sub> and CH<sub>4</sub> concentration measurements, while covariance was considered zero. The variance of each measurement was calculated according to the technical standard norm NBR-14903. This analysis yielded an average standard deviation of 1% of the CO measurement.

$$i = \sqrt{\left(\frac{\partial X}{\partial \text{CH}_{4_e}}\right)^2 * i_{\text{CH}_{4_e}}^2 + \left(\frac{\partial X}{\partial \text{CO}_e}\right)^2 * i_{\text{CO}_e}^2 + \left(\frac{\partial X}{\partial \text{CO}_{2_e}}\right)^2 * i_{\text{CO}_{2_e}}^2 + \dots} \quad (11)$$

$$\sqrt{\dots + \left(\frac{\partial X}{\partial \text{CH}_{4_s}}\right)^2 * i_{\text{CH}_{4_s}}^2 + \left(\frac{\partial X}{\partial \text{CO}_s}\right)^2 * i_{\text{CO}_s}^2 + \left(\frac{\partial X}{\partial \text{CO}_{2_s}}\right)^2 * i_{\text{CO}_{2_s}}^2}$$

#### 4. Model parameter estimation and validation

Based on the kinetic expressions, the development of a fundamental model to describe the shift reactor behavior represents an important tool for in-depth studies and performance optimization.

For modeling purposes, the experimental data set was firstly modeled considering a model with a reasonable amount of simplifying hypothesis and literature reported parameters. Afterwards, some of the hypotheses need to be disregarded, allowing an increase in model complexity, leading to further parameter estimation. Different hypotheses were disregarded until the model could successfully describe the experimental data set behavior. Only steady-state analysis was performed.

Parameter estimation was performed using a simplex-based method (Himmelblau et al., 2002) focusing on minimizing the classical least square objective function based on the difference between experimental and predicted CO conversion values. The experimental industrial data set was divided into two groups, the first for parameter estimation and the second for model validation.

Despite the relaxation of some simplifying hypotheses, in all models, both axial and radial diffusion were not considered. This choice occurred due to some features of the studied reactor, for example, it presents a high length to diameter ratio, in order to assure a turbulent flow for different operating conditions. Consequently, effects of a possible external diffusive resistance tend to be reduced. A second common simplifying hypothesis present in all models concerns the absence of pressure drop, therefore an isobaric reactor was considered. This hypothesis was assumed because experimental data revealed a pressure drop less than 3% along the catalyst bed, bellow literature recommendation threshold of 10% to disregard possible pressure drop effects (Iordanidis, 2002).

##### 4.1 Model 1 – Pseudo-homogeneous isothermal reactor

The first modeling attempt represents a very simplified reactor model as given by Eq. (12)

$$\frac{dX_a}{dz} = \frac{r_a \cdot \rho_B \cdot S}{F_{a0}} \quad (12)$$

The reaction rate is based on power law kinetics and is given by Eq. (13)

$$r_a = F_{PRESS} \cdot k_0 \cdot e^{\frac{-Ea}{RT}} \cdot y_{CO}^l \cdot y_{H2O}^m \cdot y_{CO2}^n \cdot y_{H2}^q \cdot \left( 1 - \frac{1}{K_{eq}} \cdot \frac{y_{CO2} \cdot y_{H2}}{y_{CO} \cdot y_{H2O}} \right) \quad (13)$$

For modeling purposes, reaction rate considered molar fractions instead of the components partial pressure, according to (Adams & Barton, 2009). According to the authors, a pressure correction factor,  $F_{press}$ , given by Eq. (14) also needs to be considered as a pressure increase tends to increase the effect of molecular diffusion inside the catalyst pore.

$$F_{PRESS} = P^{\left(0.5 - \frac{P}{250}\right)} \quad (14)$$

where:  $P$  is the absolute pressure in bar.

The equilibrium constant,  $K_{eq}$ , is given by Eq. (15), obtained by considering temperature dependent heat capacities.

$$\ln(K_{eq}) = \frac{5693,5}{T} + 1,077 \cdot \ln(T) + 5,44 \cdot 10^{-4} \cdot T - 1,125 \cdot 10^{-7} \cdot T^2 - \frac{49170}{T^2} - 13,148 \quad (15)$$

Finally, it is worth mentioning that the reaction rate constants were obtained from (Hla et al., 2009) as presented in Table 4.1.1 and also that the catalyst activity was considered constant.

$k_0$	$E_a$	$l$ CO	$m$ H <sub>2</sub> O	$n$ CO <sub>2</sub>	$q$ H <sub>2</sub>
700	111	1.0	0	- 0.36	- 0.09

Table 4.1.1 - Reaction rate exponents.

After solving the reactor model, normalized experimental CO conversion plotted against normalized CO conversion predicted values are shown in Figure 4.1.1. It can be observed that a systematic deviation occurs, probably because of the number of simplifying assumptions. The first hypothesis to be revisited is the reactor isothermal behavior, mainly because of the direct temperature effect on CO conversion and also because of the reaction exothermal behavior.

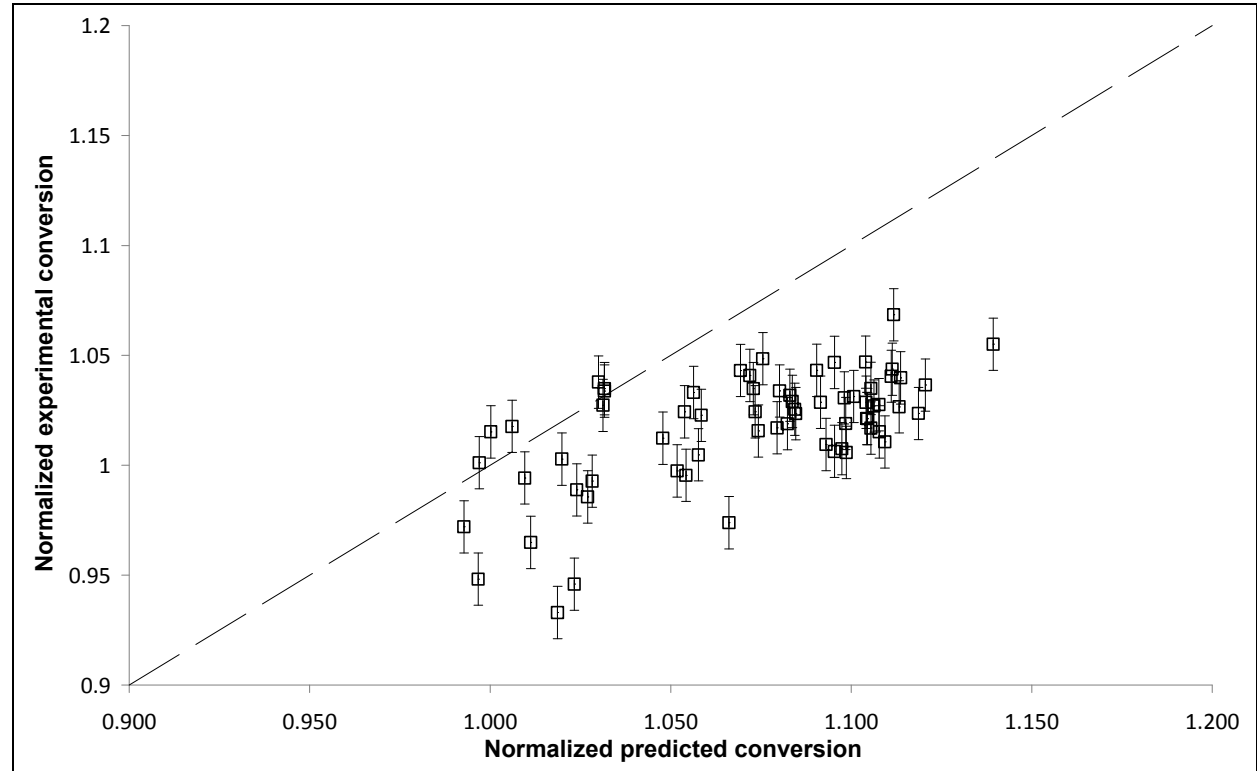


Fig. 4.1.1. Model 1 results.

#### 4.2 Model 2 – Pseudo-homogeneous non-isothermal reactor

This model represents an extension of Model 1. Due to the non-isothermal behavior, the reaction rate is not constant along the reactor length. The exothermal characteristic of the reaction also contributes to performing a heat balance on the reactor, yielding Eq. (16):

$$\sum F_j \cdot c_{pj} \cdot \frac{dT}{dz} = (-\Delta H_R) \cdot r_a \cdot \rho_B \cdot S \quad (16)$$

Consequently, the reactor model is now comprised by a system of ordinary differential equations. Figure 4.2.1 is obtained after plotting normalized experimental CO conversion against normalized CO conversion predicted values. It can be observed, after comparison with Figure 4.2.1, that non-isothermal feature actually resulted in worse model predictions. By analyzing Figure 7, it can be observed that for higher experimental conversion values, systematic higher predictions are obtained. This probably happens because the non-isothermal behavior leads to higher temperature values, consequently not only leading to higher reaction rates overestimating CO conversion, but also affecting diffusion phenomena inside the catalyst particles. Therefore, an alternative modeling approach would be considering an effectiveness factor in order to correct the reaction rate.

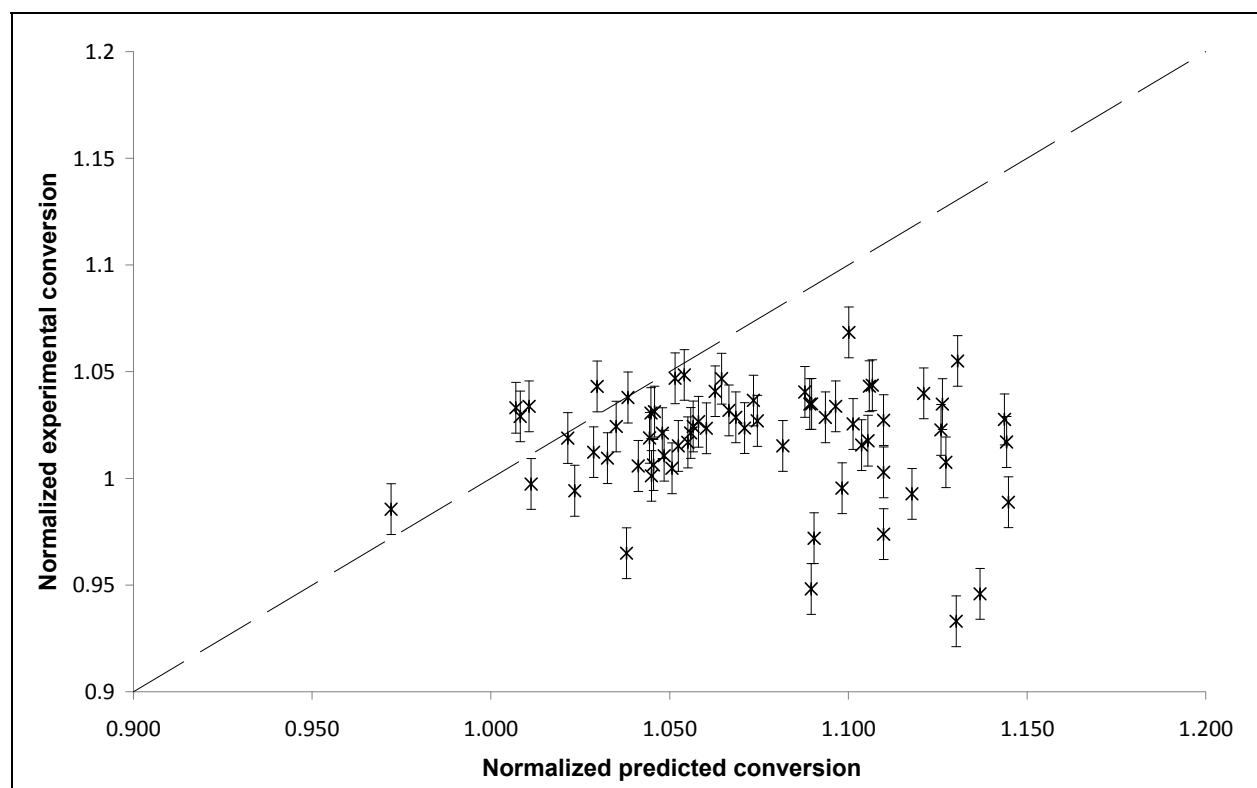


Fig. 4.2.1. Model 2 results.

#### 4.3 Model 3 – Pseudo-homogeneous non-isothermal reactor with reaction rate correction

In this model, the reaction rate (Eq. 13) is corrected by an effectiveness factor as presented by Eq. (17).

$$r_{a\text{-effective}} = \eta \cdot r_a \quad (17)$$

It is important to realize that in Model 1 and Model 2 only simulation studies were carried out, no model parameter estimated. Now, parameter  $\eta$ , which remains in the interval (0,1], will be estimated in order to improve data fitting the model predictions. As mentioned before, only part of the experimental data set will be used for parameter estimation using the minimum least square method, while the other part will be used for validation purposes.

After parameter estimation, an optimal value of  $\eta = 0.56$  was obtained. Considering this value, the mathematical model was then used to predict CO conversion as presented in Figure 4.3.1. It can be seen a considerable improvement in the model prediction, which was achieved by estimating only one parameter. However, the experimental data set refers to a considerable production horizon; consequently, catalyst activity may have changed, leading to another opportunity for model improvement.

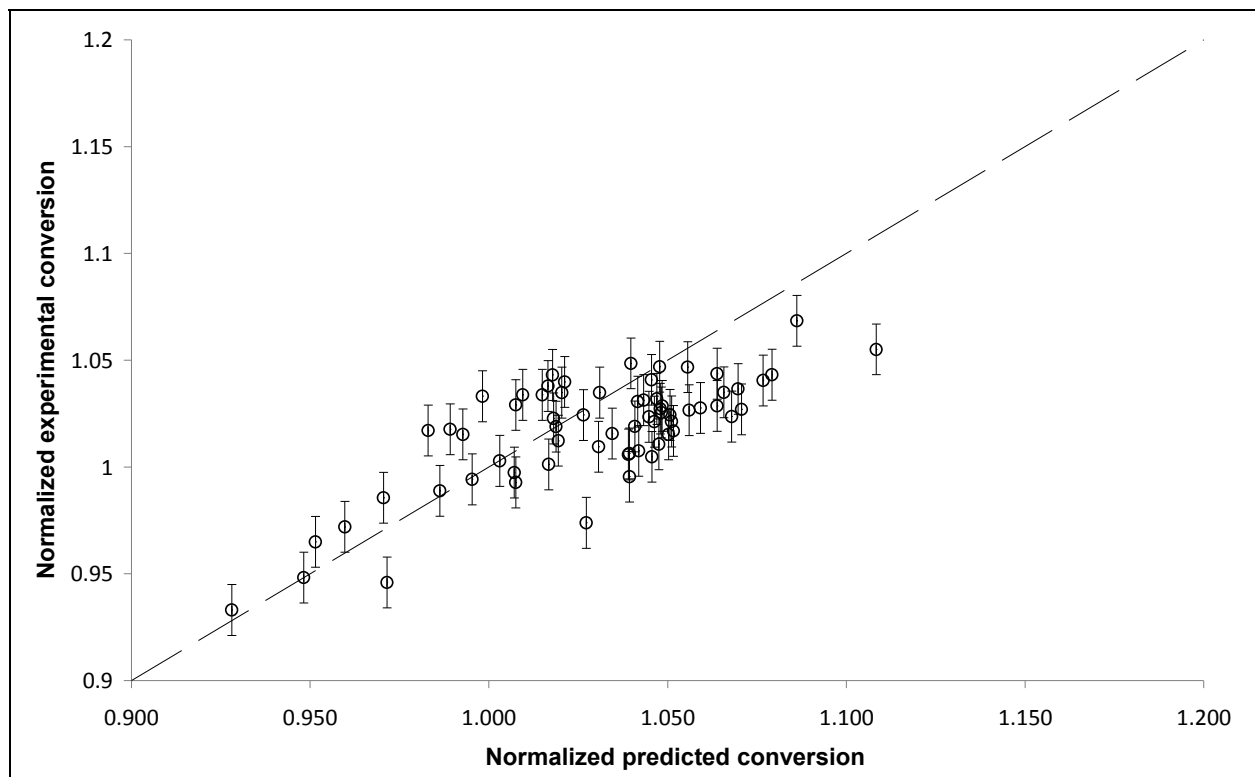


Fig. 4.3.1. Model 3 validation.

#### 4.4 Model 4 – Pseudo-homogeneous non-isothermal reactor with reaction rate correction and catalyst deactivation

This model considers the reaction rate given by Eq. (18)

$$r_{a\text{-effective}} = \eta \cdot a(t) \cdot r_a \quad (18)$$

In this effective reaction rate, the catalyst activity,  $a(t)$ , can be described by a hyperbolic rate expression (Eq. (19)) as previously reported (Keiski et al., 1992):

$$a(t) = \frac{1}{(1 + \alpha \cdot t)^{1/3}} \quad (19)$$

It must be stressed that  $\alpha$  is the only parameter to be estimated in Model 4 as  $\eta$  was kept equal to 0.56. Parameter  $\alpha$  was estimated as  $10^{-5}$ . Figure 4.4.1 presents experimental normalized CO conversion plotted against predicted normalized values considering only the validation data set. It can be observed that the use of catalyst deactivation improved model performance, indicating an important role played by catalyst deactivation. However, the intrinsic reaction rate was not yet used for parameter estimation as exponents  $i$ ,  $m$ ,  $n$ ,  $p$  values were considered the ones reported in the literature (see Table 4.1.1), consequently, this creates an alternative for model improvement.

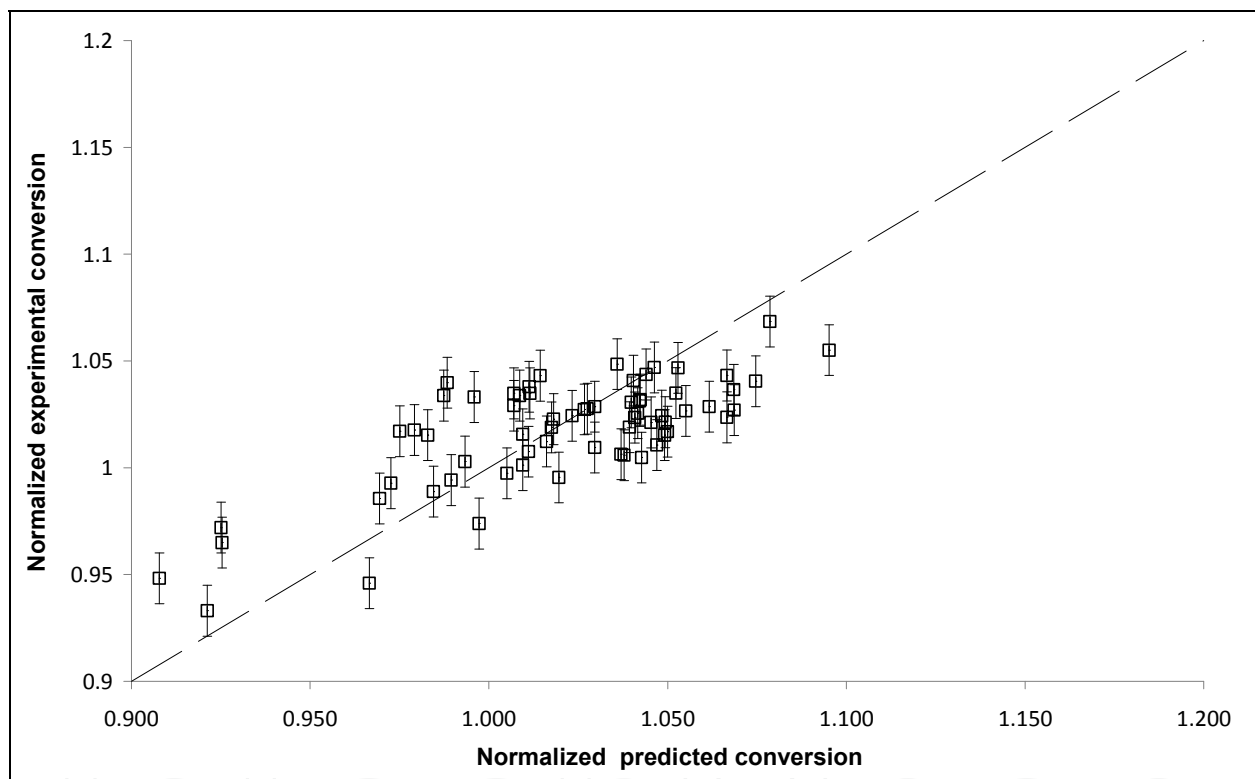


Fig. 4.4.1. Model 4 validation.

#### 4.5 Model 5 – Revisiting model 4 intrinsic reaction rate

It can be observed that the order of H<sub>2</sub>O in the reaction rate is equal to 0 as reported in Table 4.1.1. This indicates that H<sub>2</sub>O is present in such a large excess that concentration changes does not considerably affect the reaction rate (Hla et al., 2009). However, in the industrial reactor, where the feed composition may change due to the nature of a petrochemical plant, H<sub>2</sub>O may be in excess, but not in enough amount to be considered constant throughout the reactor length. Therefore, exponent  $m$  needs to be re-estimated, while the others will be kept at the same values. However, changes in  $m$  may affect the effective rate, consequently,  $\eta$  value also needs to be revisited and estimated. To sum up, Model 5 basically keeps the same structure of Model 4 only different parameters need to be estimated.



After performing the estimation task, a  $m$  value of 0.2 was obtained, simultaneously to a  $\eta$  value equal to 0.575. Figure 4.5.1 presents experimental and predicted values of CO conversion, showing that model predictions improved considering the new  $m$  value.

In order to compare the model predictions, the sum of the square difference of experimental and predicted values of CO conversion was performed and Model 2 led to the highest sum being the worst model. The sum of the squares of Model 2 was used as normalization factor and the normalized sum of all models are presented in Figure 4.5.2. It can be concluded that two hypotheses played a key role in the reactor modeling: firstly the isothermal behavior; secondly, the effectiveness factor. Further changes were import to improve, but not considerably, the data fit. It must also be noted that a few number of parameters were estimated, indicating an important likelihood feature of the reactor model. Finally, it is worth stressing that the correlation coefficient between experimental data and model predictions of Model 5 was equal to 0.8.

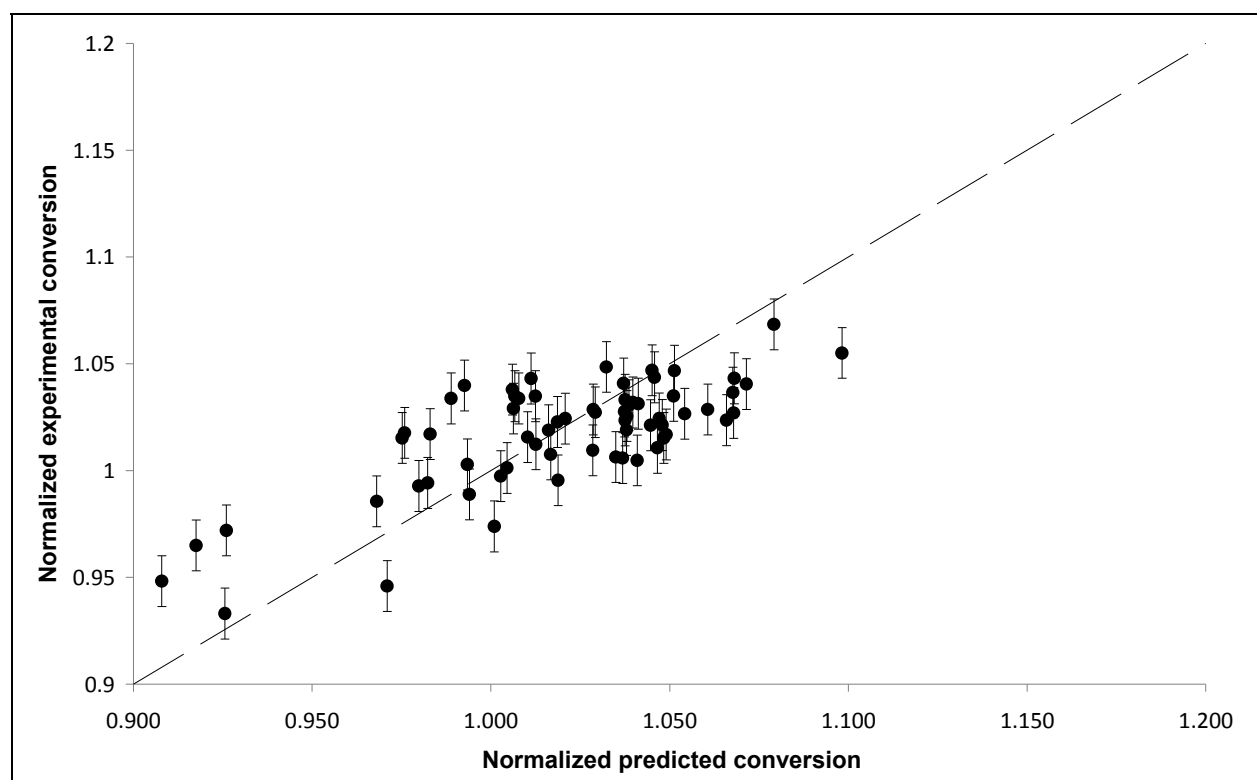


Fig. 4.5.1. Model 5 validation.

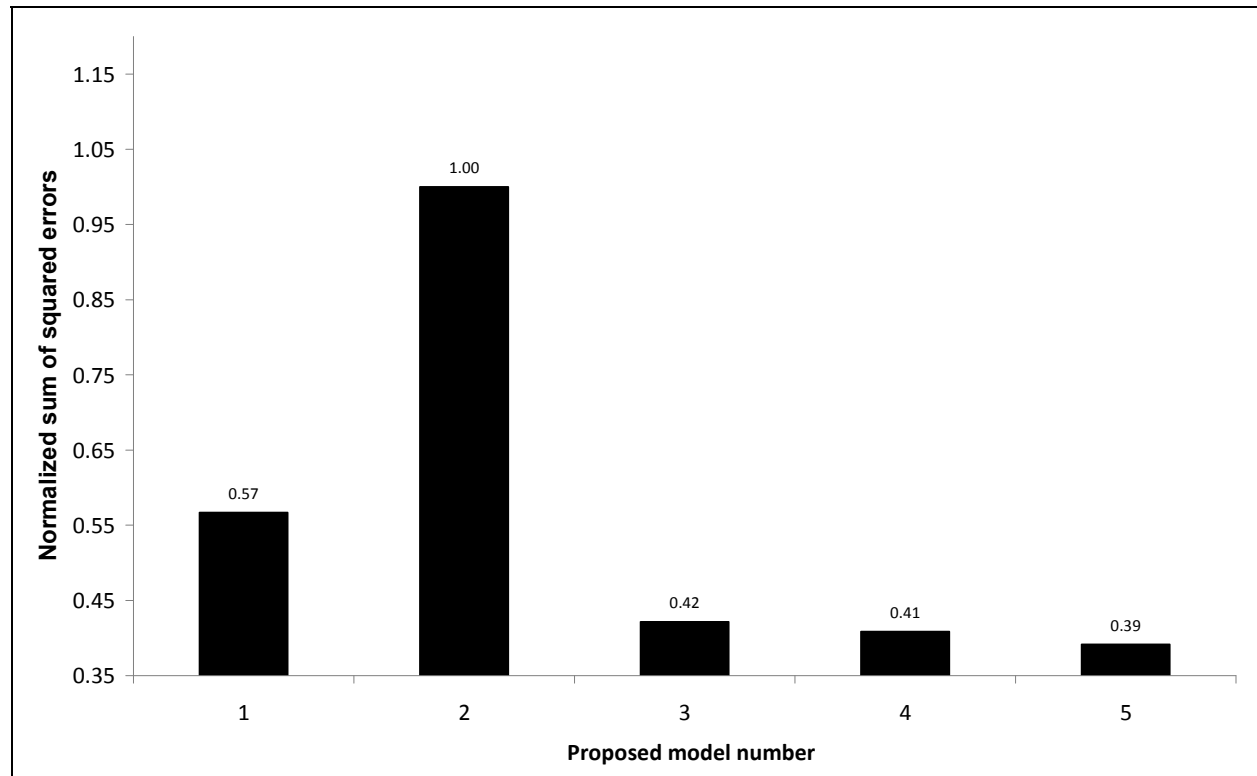


Fig. 4.5.2. Model comparison.

## 5. A novel approach to optimal process control strategy

Due to the shift reaction features, for a given reactor feed stream composition and flow rate, the temperature of the feed stream can be manipulated in order to maximize CO conversion. Consequently, if the industrial reactor has in-line/on-line composition analyzers as well as flow rate measurement instrumentation, on-line optimization can be successfully implemented. The problem is that this kind of in-line/on-line instrumentation is not only expensive but also may need continuous and excessive calibration and maintenance. Therefore, some question arises: can other real-time measurements be used for CO conversion? How does temperature influence CO conversion correlated? This is an important issue as temperature measurements are usually reliable, accurate, real-time and low cost. Moreover, fixed bed reactors can have temperature instruments installed along the reactor length, providing a temperature profile. Towards this, a novel and alternative approach will be presented in order to overcome this issue, focusing on CO conversion control.

Figure 5.1 presents historical normalized CO conversion data plotted against normalized feed flow-rate values, obtained from PETROBRAS shift reactor unit. As mentioned before, the normalized variables equal to 1 represent the reactor design values. These data refer to the same reactor temperature; however, due to the nature of petrochemical process, raw material composition can fluctuate, explaining the different CO conversion values obtained for the same experimental conditions. As expected, the higher the feed flow rate, the lower the reactor conversion.

In Figure 5.1, one observes, for example, conversions of 1.02 or 1.04, indicating that in these scenarios the experimental values were over the design values. The same observation can be made for the feed flow rate, indicating some operating conditions either bellow or above the design values. Consequently, it is important to emphasize that the reactor feed composition represents an important disturb variable affecting reactor performance, enhancing the importance of well tuned and designed regulatory control loops.

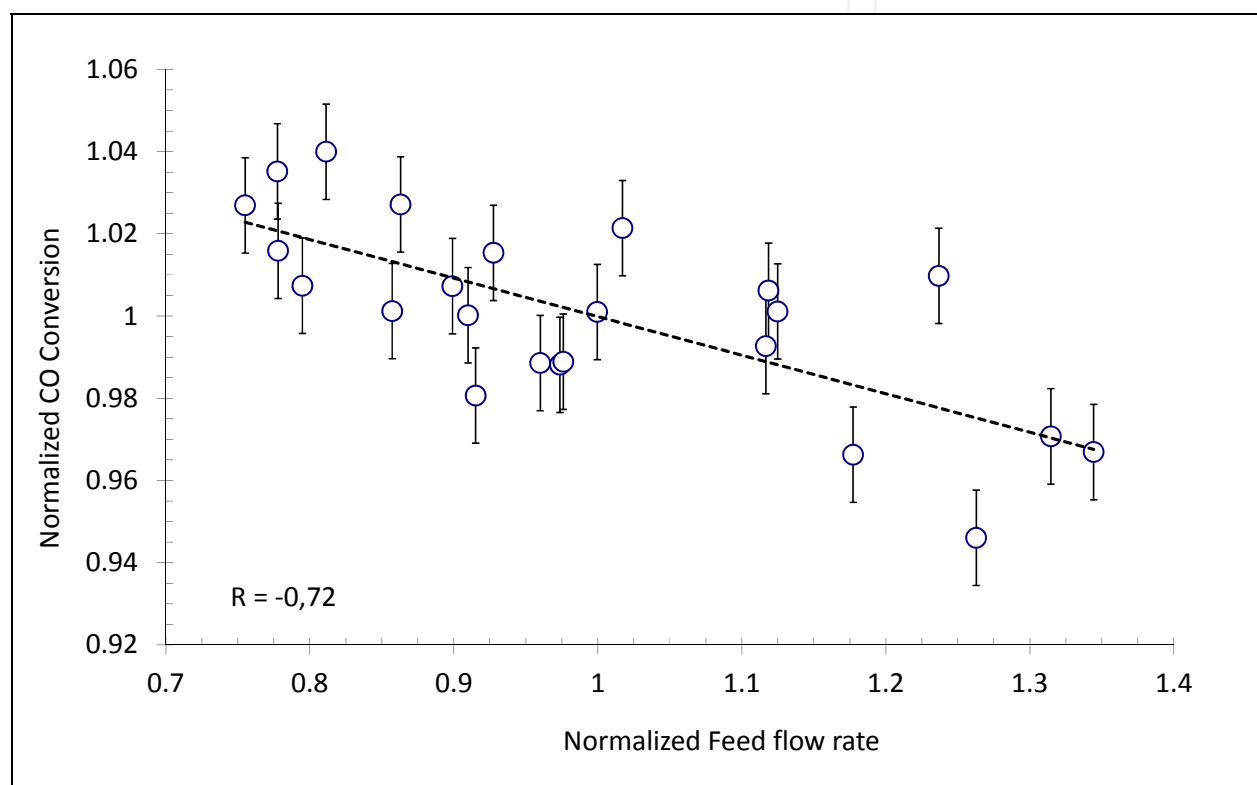


Fig. 5.1. Historical data: CO Conversion versus feed flow rate.

The studied shift reactor has thermocouples installed at the reactor feed and exit streams. It also has four thermocouples equally distributed along the reactor bed. After performing extensive sensitivity analysis, the temperature difference between the thermocouple placed on the reactor exit stream and last thermocouple of the bed provided the highest sensitivity, here denominated  $\Delta T$ . After analyzing the historical data set, Figure 5.2 presents experimental data of CO conversion plotted against normalized  $\Delta T$ . It can be observed a good correlation between both variables, which corroborate the idea of monitoring CO conversion by using lower cost measurements. Finally, Figure 5.3 presents the relationship between normalized  $\Delta T$  and normalized feed flow rate values, as expected indicating strong correlation and also good sensitivity.

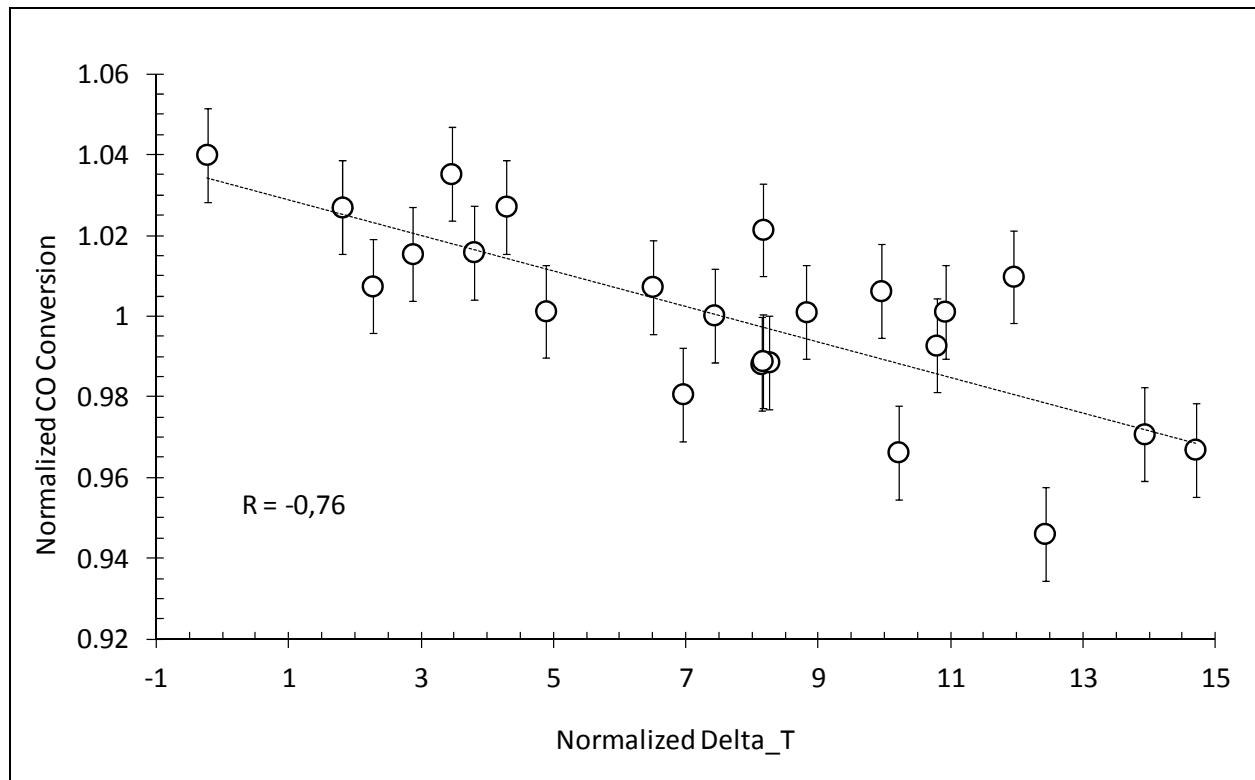


Fig. 5.2. Historical data: CO Conversion versus Delta\_T.

The developed mathematical model was used for sensitivity analysis in order to study the CO conversion behavior for different operating conditions. More specifically, this analysis is aimed at providing not only the control feasibility itself, but also the feasibility of leading to operating conditions which may allow optimum conversion values. Figure 5.4 shows the CO conversion behavior for different feed flow rate values, considering in all simulations the feed composition design value. More specifically, the design value of the feed flow rate (FLOW1), the design value increased by 35% (FLOW2) and the design value increased by 55% (FLOW3) were used. Firstly, one can observe that due to the shape of the curve, the feed flow rate temperature can be manipulated in order to reach a maximum CO conversion. Secondly, the simulation results show that keeping the reactor feed temperature constant, for example at 1.03, an increase in the flow rate may lead CO conversion reduction, similar to the behavior of the historical data exhibited by Figure 5.1. It is also important to observe the effect of the temperature of the reactor feed stream on the CO conversion. After careful analysis, it can be also noted that to keep track of CO conversion, for example, at 0.955, the feed flow rate needs to be increased for a feed stream temperature increase. Consequently, feed flow rate and feed temperature can be regarded as important manipulated variables for CO conversion either in servo or regulatory control.

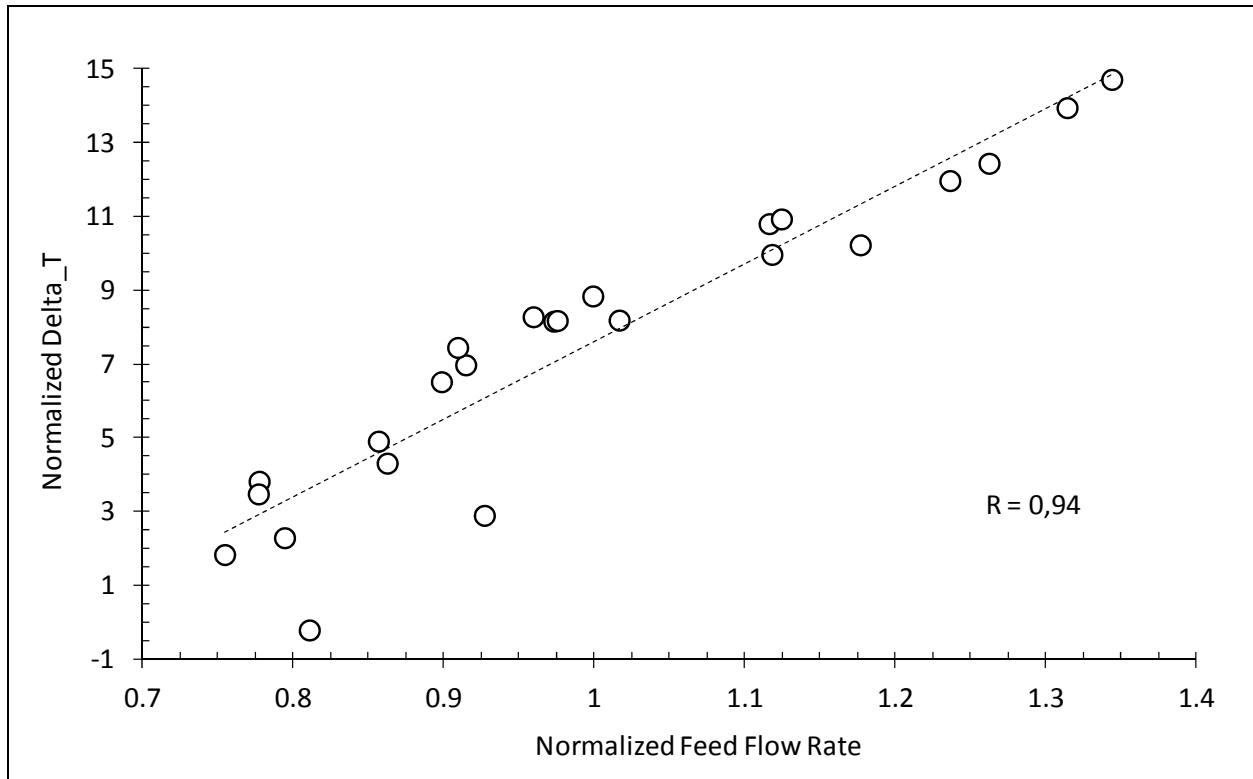


Fig. 5.3. Historical data: Delta\_T versus feed flow rate.

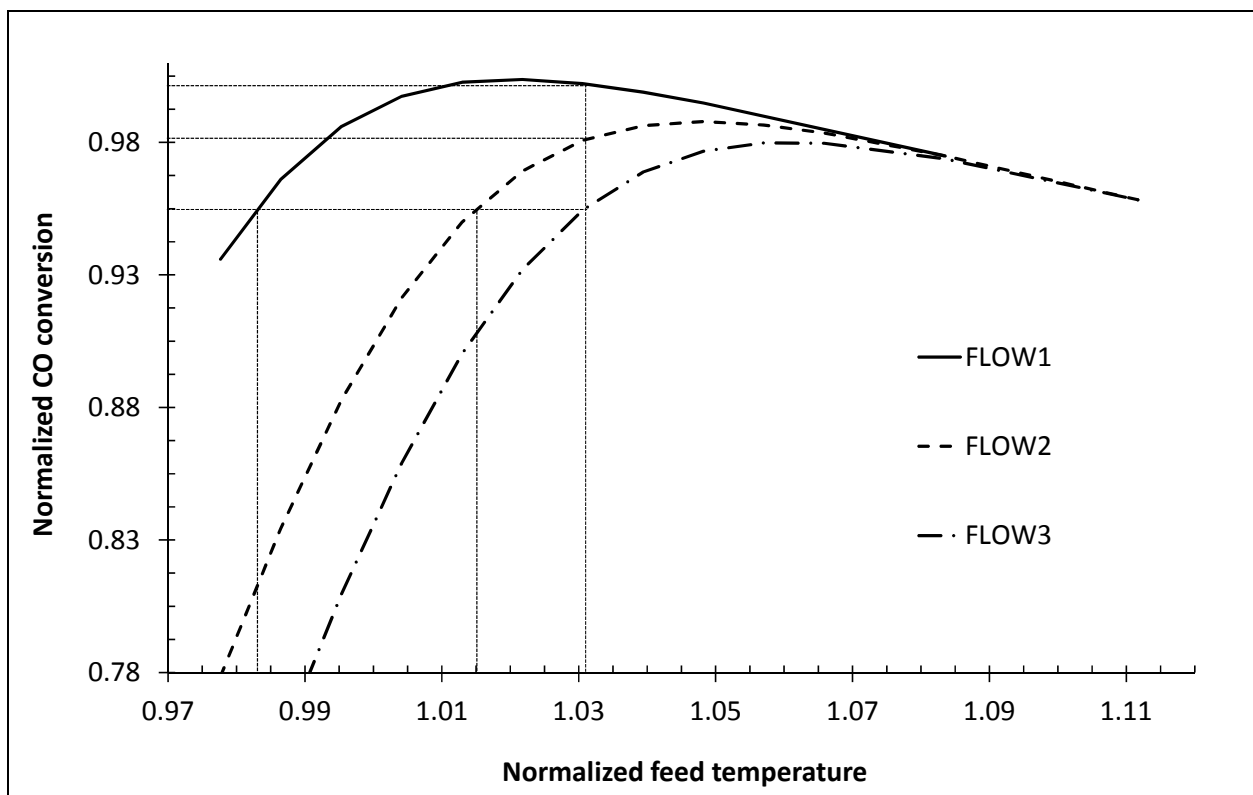


Fig. 5.4. Sensitivity Analysis.

However, it is important not only to provide control feasibility, but also to assure that the control can lead to optimal conversion values. Figure 5.5 presents a sensitivity analysis study focusing on the effect of feed composition. The reactor feed flow rate was kept constant in all simulations, while two different feed compositions were chosen, more specifically, the design feed composition (COMP1) and a feed composition involving an increase in CO amount (COMP2). For each feed composition, the temperature of the feed stream was changed in order to evaluate the correspondent resulting Delta\_T values and the maximum conversion was determined and plotted. For COMP1, the maximum conversion is reached at a Delta\_T value equal to roughly 3.7. Consequently, for this feed composition and feed flow rate, the feed temperature set-point needs to be roughly 1.01. The same analysis can be performed for composition 2.

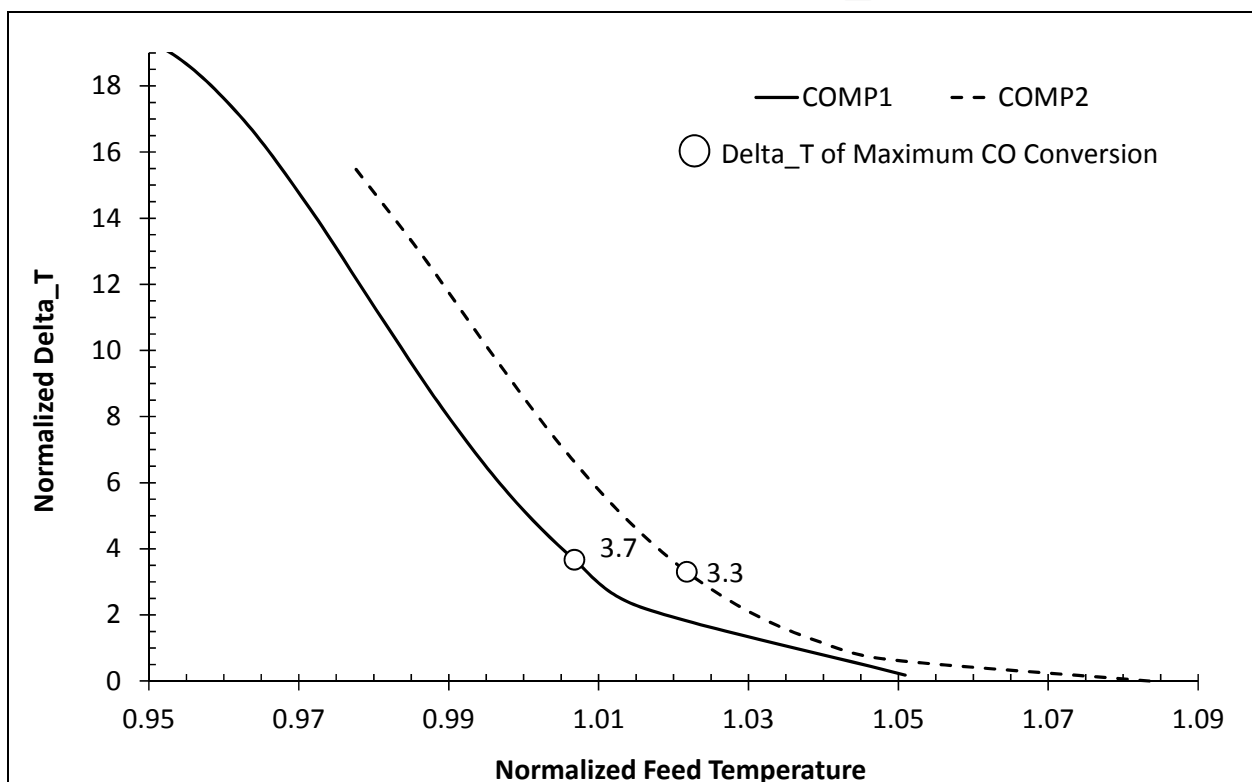


Fig. 5.5. Sensitivity Analysis: Composition.

On the other hand, Figure 5.6 presents a sensitivity analysis study focusing on the effect of feed flow rate. The reactor feed composition was set equal to COMP2 and different values of the flow rate, FLOW1, FLOW2, FLOW3 were chosen. For each feed flow rate value, the temperature of the feed stream was changed in order to evaluate the correspondent resulting Delta\_T values. For each feed flow rate, the maximum conversion was also determined and plotted. Considering the feed composition COMP2, for the feed flow rate close to the design value, Delta\_T should be equal to 3.3 to lead to the maximum CO conversion, consequently, the feed temperature set-point should be roughly 1.02. Keeping the composition unchanged and increasing the flow rate by 35%, Delta\_T should be equal to 3.6 and, therefore, the feed temperature should be increased to approximately 1.05. Increasing the design value of the feed flow rate by 55%, Delta\_T should be changed to 4.4, so the feed temperature should be increased to approximately 1.06.

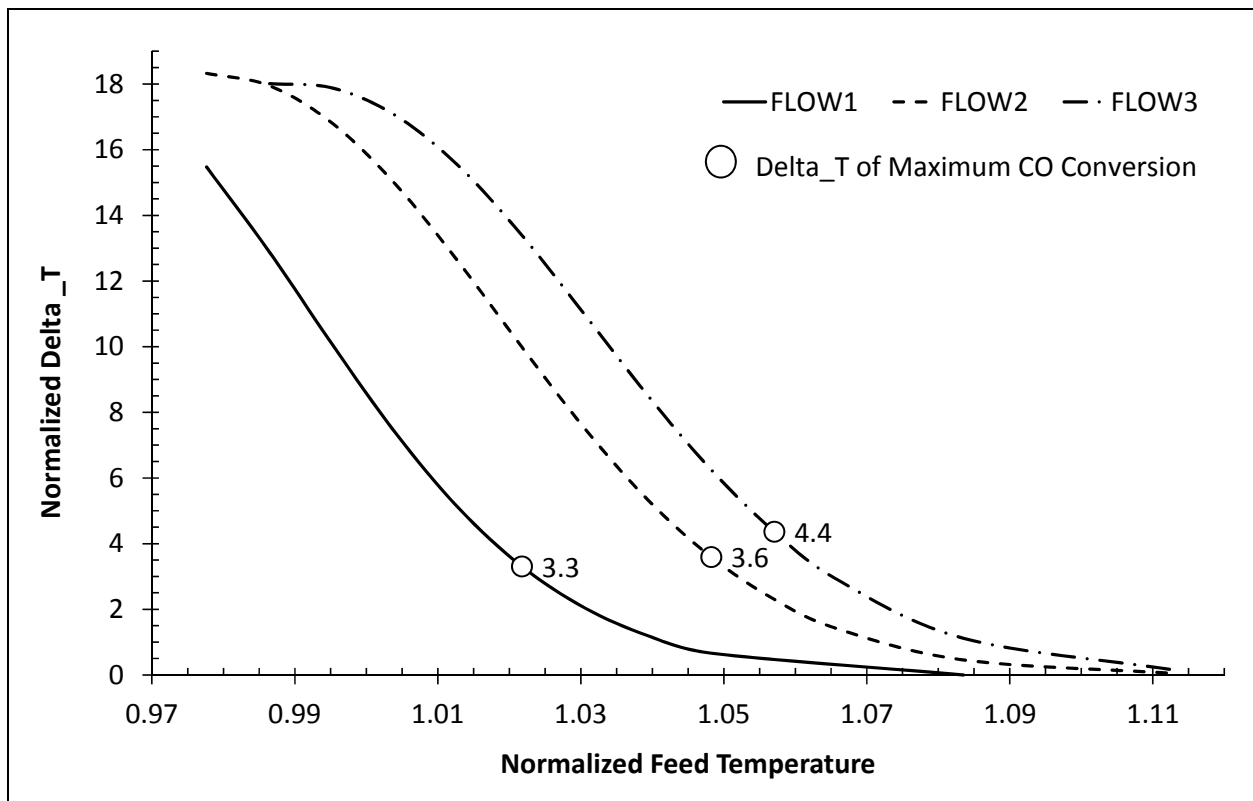


Fig. 5.6. Sensitivity Analysis: Feed Flow.

Based on the historical data and on the sensitivity analysis results, an alternative CO conversion control loop having the following features arises:

- controlling Delta\_T represents the same as controlling CO conversion;
- controlling Delta\_T can lead to optimal conversion values;
- cascade structure can be used with Delta\_T control mastering the loop by providing appropriate set-points to the reactor feed temperature control loop;
- feedforward features may also be considered as if feed flow rate changes the Delta\_T value leading to the optimal conversion needs to be updates as observed in Figure 7;
- feedforward features may also be considered if feed analyzers can be installed, as any change in feed composition would lead to a different Delta\_T set-point.

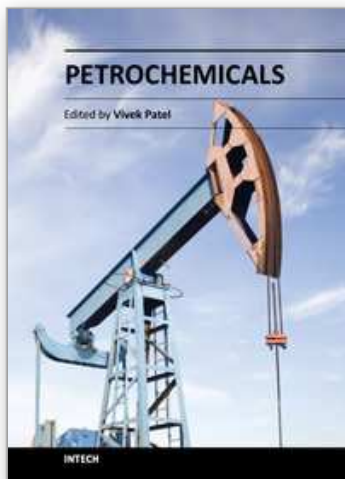
## 6. References

- Adams II, Thomas A. and Barton, Paul I. (2009). *A dynamic two-dimensional heterogeneous model for water gas shift reactors*. International Journal of Hydrogen Energy 34, 8877-8891.
- Borges, Joana Lopes. (2009). *Diagrama de fontes de hidrogênio*. Dissertação de Mestrado em Tecnologia de Processos Químicos e Bioquímicos. Universidade Federal do Rio de Janeiro. Rio de Janeiro. Brasil.
- Chen, Wei-Hsin et al. (2008). *An experimental study on carbon monoxide conversion and hydrogen generation from water gas shift reaction*. Energy Conversion and Management 49, 2801-2808.



- Edgar, Himmelblau and Lasdon. (2001). *Optimization of Chemical Processes*. 2nd Edition. New York - McGraw-Hill, pp. 10-11.
- Froment, Gilbert F. and Bischoff, Kenneth B. (1990). *Chemical reactor analysis and design*. John Wiley and Sons, ISBN 0-471-51044-0, second edition, pp. 403-404.
- Hla, San Shwe et al. *Kinetics of high-temperature water-gas shift reaction over two iron-based commercial catalysts using simulated coal-derived syngases*. *Chemical Engineering Journal* 146 (2009) 148-154.
- Iordanidis, A. A. (2002). *Mathematical Modeling of Catalytic Fixed Bed Reactors*. Ph.D. thesis, University of Twente. ISBN 9036517524, Enschede, The Netherlands.
- Keiski, R. L. et al. (1992). *Deactivation of the high-temperature catalyst in nonisothermal conditions*. *Applied Catalysis A: General*, Vol. 87, pp 185-203.
- NBR 14903 (2002) Gás Natural - *Determinação da composição por cromatografia gasosa*. Associação Brasileira de Normas Técnicas.
- Newsome, David S. (1980). *The water-gas shift reaction*. *Catal. Rev. Sci. Eng.*, 21(2), 275-318.
- Singh, C. C. P. and Saraf, D. N. (1977). *Simulation of high-temperature water-gas shift Reactors*. *Ind. Eng. Chem. Process Des. Dev.*, Vol. 16, No. 3, 313-319.
- Smith, Byron R. J. et al. (2010). *A review of the water gas shift reaction kinetics*. *International Journal of Chemical Reactor Engineering* Vol. 8, Review R4, ISSN 1542-6580.

IntechOpen



## **Petrochemicals**

Edited by Dr Vivek Patel

ISBN 978-953-51-0411-7

Hard cover, 318 pages

**Publisher** InTech

**Published online** 28, March, 2012

**Published in print edition** March, 2012

The petrochemical industry is an important constituent in our pursuit of economic growth, employment generation and basic needs. It is a huge field that encompasses many commercial chemicals and polymers. This book is designed to help the reader, particularly students and researchers of petroleum science and engineering, understand the mechanics and techniques. The selection of topics addressed and the examples, tables and graphs used to illustrate them are governed, to a large extent, by the fact that this book is aimed primarily at the petroleum science and engineering technologist. This book is must-read material for students, engineers, and researchers working in the petrochemical and petroleum area. It gives a valuable and cost-effective insight into the relevant mechanisms and chemical reactions. The book aims to be concise, self-explanatory and informative.

### **How to reference**

In order to correctly reference this scholarly work, feel free to copy and paste the following:

Douglas Falleiros Barbosa Lima, Fernando Ademar Zanella, Marcelo Kaminski Lenzi and Papa Matar Ndiaye (2012). Modeling and Simulation of Water Gas Shift Reactor: An Industrial Case, Petrochemicals, Dr Vivek Patel (Ed.), ISBN: 978-953-51-0411-7, InTech, Available from:

<http://www.intechopen.com/books/petrochemicals/modeling-and-simulation-of-water-gas-shift-reactors-an-industrial-case>

**INTECH**  
open science | open minds

### **InTech Europe**

University Campus STeP Ri  
Slavka Krautzeka 83/A  
51000 Rijeka, Croatia  
Phone: +385 (51) 770 447  
Fax: +385 (51) 686 166  
[www.intechopen.com](http://www.intechopen.com)

### **InTech China**

Unit 405, Office Block, Hotel Equatorial Shanghai  
No.65, Yan An Road (West), Shanghai, 200040, China  
中国上海市延安西路65号上海国际贵都大饭店办公楼405单元  
Phone: +86-21-62489820  
Fax: +86-21-62489821

© 2012 The Author(s). Licensee IntechOpen. This is an open access article distributed under the terms of the [Creative Commons Attribution 3.0 License](#), which permits unrestricted use, distribution, and reproduction in any medium, provided the original work is properly cited.

IntechOpen

IntechOpen